

**Thermal management of electronic components  
using nano-enhanced phase change material  
(NePCM)**

**A project report**

*Submitted in partial fulfillment of the  
requirements for the award of the degree*

*of*

**BACHELOR OF TECHNOLOGY**

**IN**

**MECHANICAL ENGINEERING**

*Submitted by*

**Vaidya Dattaraj Vilas (150003036)**

**Vinay Shelke (150003037)**

**Under the Supervision of**

**Dr. Santosh K. Sahu**



**Indian Institute of Technology Indore**

**November 2018**

## **CANDIDATE'S DECLARATION**

We hereby declare that the project entitled “**Thermal management of electronic components using nano-enhanced phase change material (NePCM)**” submitted in partial fulfillment for the award of the degree of Bachelor of Technology in ‘Mechanical Engineering’ completed under the supervision of **Dr. Santosh K. Sahu, Associate Professor, IIT Indore** is an authentic work.

Further, we declare that we have not submitted this work for the award of any other degree elsewhere.

**Vaidya Dattaraj Vilas (150003036)**

**Date**

**Vinay Shelke (150003037)**

---

## **CERTIFICATE by BTP Guide**

It is certified that the above statement made by the students is correct to the best of my knowledge.

**Signature**

**Dr. Santosh K. Sahu  
Associate Professor,  
Mechanical Engineering,  
IIT Indore**

## **Preface**

*This report on “Thermal management of electronic components using nano-enhanced phase change material (NePCM)” is prepared under the guidance of Dr. Santosh K. Sahu.*

*The effect of dispersion of nanoparticles on the thermal performance of heatsinks containing phase change material (PCM) has been analyzed. Experiments have been carried out with various weight fractions of nanoparticles and different geometries of heatsinks with plate fins.*

*The results obtained from the present experimental study are presented in the tabular and graphical form.*

**Vaidya Dattaraj Vilas (150003036)**

**Vinay Shelke (150003037)**

B.Tech. IV Year  
Discipline of Mechanical Engineering  
IIT Indore

## **Acknowledgments**

First and foremost, we would like to thank our supervisor Dr. Santosh K. Sahu for guiding us thoughtfully and efficiently throughout this project, giving us an opportunity to work at our own pace while providing us with useful directions whenever necessary. We would like to thank Mr. Rohit Kothari (Ph.D. scholar) for his constant support and contribution throughout the project. We would also like to thank Dr. P. Maheandera Prabu, Mr. Vishal V. Nirgude, Mr. Avadhesh Kumar Sharma, Mr. Saurabh Yadav, Mr. Pushpanjay Singh and Mr. Anuj Kumar for their invaluable support and guidance. We would also like to express gratitude towards the staff members of Fluid Mechanics and Machinery, Advanced Manufacturing Process, Mechatronics and Instrumentation Laboratory and Central workshop for helping us wholeheartedly along the way.

The financial support provided by the **Indian Institute of Technology Indore** and **Department of Science and Technology (DST)** under the project grant DST/TMD/MES/2k17/65 is gratefully acknowledged.

We would like to take this opportunity to thank our fellow batch mates for being great sources of motivation and for providing encouragement throughout the length of this project.

Finally, we offer our sincere thanks to all other persons who knowingly or unknowingly helped us in completing this project.

**Vaidya Dattaraj Vilas (150003036)**

**Vinay Shelke (150003037)**

B.Tech. IV Year  
Discipline of Mechanical Engineering  
IIT Indore

## Abstract

Present experiment focuses on implementing passive cooling thermal management technique using heatsinks filled with paraffin wax as phase change material in which  $\text{Al}_2\text{O}_3$  nanoparticles are dispersed as thermal conductivity enhancer (TCE) in different weight fractions( $\phi$ ) for improved performance. Unfinned, finned (No. of fins =1 & 2) heatsinks of dimensions  $100 \times 100 \times 20 \text{ mm}^3$  are used in this investigation. Experimental analysis is performed on the different configurations of heatsinks and nano-enhanced phase change materials (NePCM) consisting various weight fraction of  $\text{Al}_2\text{O}_3$  nanoparticles ( $\phi=0\%$ ,  $0.5\%$ ,  $4\%$ , and  $6\%$ ) for a constant heat flux of  $2.0 \text{ kW/m}^2$ . Results show that latent heat decreases with increase in the  $\text{Al}_2\text{O}_3$  nanoparticle loading. Addition of  $\text{Al}_2\text{O}_3$  nanoparticles in the PCM results in the reduced melting time of PCM. While pure PCM based heatsink keeps heatsink temperature lower for longer time duration. Hence, the use of pure PCM based heatsink will be advisable in continuous operating electronic devices. However, NEPCM based heatsink will perform better in intermittent operating electronic devices, where power spikes are unavoidable.

## Table of content

<b>CANDIDATE’S DECLARATION</b> .....	II
<b>CERTIFICATE by BTP Guide</b> .....	II
<b>Preface</b> .....	III
<b>Acknowledgments</b> .....	IV
<b>Abstract</b> .....	V
<b>Chapter 1: Introduction</b> .....	1
1.1 Introduction .....	1
1.2 Classification of phase change materials (PCM).....	2
1.2.1. Inorganic PCM .....	2
1.2.2. Organic PCM.....	3
1.2.3. Eutectics .....	3
1.3 Selection criteria for PCM.....	3
1.4 Applications of PCM .....	4
1.5 Review of literature .....	5
1.6 Objective.....	8
<b>Chapter 2: Experimental Facility</b> .....	9
2.1 Preparation of Heatsinks .....	9
2.2 Locations of Thermocouples .....	11
2.3 Preparation of nano-enhanced PCM.....	12
2.4 Setup to measure the thermal performance of a heatsink filled with NePCM .....	13
<b>Chapter 3: Characterization and Data Processing</b> .....	14
3.1 DSC Characterization .....	14
3.2 SEM Characterization.....	14
3.3 Data processing.....	15
3.3.1. Calculating melt fraction.....	15

<b>Chapter 4: Results and Discussions</b> .....	18
4.1 Comparison curves .....	18
4.2 Latent Heat Variation .....	19
4.3 Propagation of melt front and variation of melt fraction with time .....	20
4.4 Effect of nanoparticle loading on heatsink base temperature .....	23
<b>Chapter 5: Conclusions</b> .....	24
<b>References</b> .....	25
<b>Publications</b> .....	27
<b>Appendix</b> .....	28

## List of Figures

Fig 1. Classification of phase change materials.....	2
Fig 2. Preparation of heatsinks.....	9
Fig.3 Photographic view of heatsinks .....	10
Fig 4. Detailed view of 1 finned heatsink.....	10
Fig 5. Detailed view of 2 finned heatsink.....	10
Fig 6. Locations of thermocouples in the heatsink. ....	11
Fig 7. Schematic diagram for the preparation of NePCM .....	12
Fig 8. Schematic diagram of the experimental setup .....	13
Fig 9. Detailed view of heatsink assembly .....	13
Fig 11. DSC curve for paraffin wax dispersed with different weight fractions of Al <sub>2</sub> O <sub>3</sub> Nanoparticles .....	14
Fig 10. DSC curve of paraffin wax.....	14
Fig 12. FESEM image of NePCM.....	15
Fig 13. Steps involved in image processing to obtain the melt fraction for unfinned heatsink .....	16
Fig 14. Steps involved in image processing to obtain the melt fraction for 2 finned heatsink	16
Fig 15. Comparison of present investigation with existing studies .....	18
Fig 16. Comparison of the base temperature of 2 finned heatsink with and without PCM.....	18
Fig 17. Variation of latent heat of PCM with nanoparticle loading.....	19
Fig 18. Progression of melt front of pure PCM ( $\phi=0$ ) for the unfinned heatsink.....	20
Fig 19. Progression of melt front of NePCM ( $\phi=4\%$ ) for the 2 finned heatsink.....	20
Fig 21. Melting time of NePCMs for the unfinned heatsink .....	21
Fig 20. Variation of melt fraction with time for the unfinned heatsink.....	21
Fig 22. Variation of melt fraction with time for the 1 finned heatsink .....	21
Fig 23. Melting time of NePCMs for the 1 finned heatsink .....	21
Fig 25. Melting time of NePCMs for the 2 finned heatsink .....	21

Fig 24. Variation of Melt fraction with time for the 2 finned heatsink.....	21
Fig 27. Variation of base temperature with time for 2 finned heatsink.....	23
Fig 26. Variation of base temperature with time for unfinned heatsink.....	23
Fig 28. Variation of base temperature with time for 1 finned heatsink.....	23

### **List of Tables**

Table 1. Thermophysical properties of Paraffin wax, TCE and Insulator.....	12
Table 2. Variation of latent heat of PCM with nanoparticle loading.....	19

# Chapter 1

## Introduction

### 1.1 Introduction

Recent technological advancements made electronic devices a key factor in our modern life. The constant need for efficiency and performance is pushing them to their limits. The world is moving from big to compact and handy products. Because of miniaturization, the temperature concentration is increasing. Higher temperature can result in a failure of a component leading to failure of the whole electronic device. Studies have shown that most of the failure caused in electronic devices are thermal related. Hence proper thermal management techniques are necessary for ensuring a long life as well as good performance.

Controlling the temperature of a system by means of technology-based thermodynamics and heat transfer is known as thermal management of the system. Thermal management techniques can be divided into two types, a) active cooling techniques and b) passive cooling techniques.

Active cooling techniques requires external power for functioning. There are many types of active cooling techniques, e.g., a) Forced air cooling, b) Cold plates, c) Synthetic jet air cooling and d) Heat pipe, etc.

Passive cooling techniques can be achieved by either geometry (finned heatsinks) or using phase change materials. The main advantage of passive cooling techniques over active is the capacity to dissipate heat and the power consumption, and the size needed. Hence passive cooling technique is chosen in this experiment. Energy absorbed as latent heat is way more than sensible heat, hence latent heat based passive cooling mechanism is more promising and efficient.

A phase change material (PCM) is a substance which has high latent heat of fusion and can store and release large amounts of energy. PCMs have various advantages such as chemical stability, high storage density and low vapor pressure at the operating temperature, a slight temperature drop during heat recovery and non-corrosiveness. Their thermo-physical properties remain same after many heating and cooling cycles.

## 1.2 Classification of phase change materials (PCM)

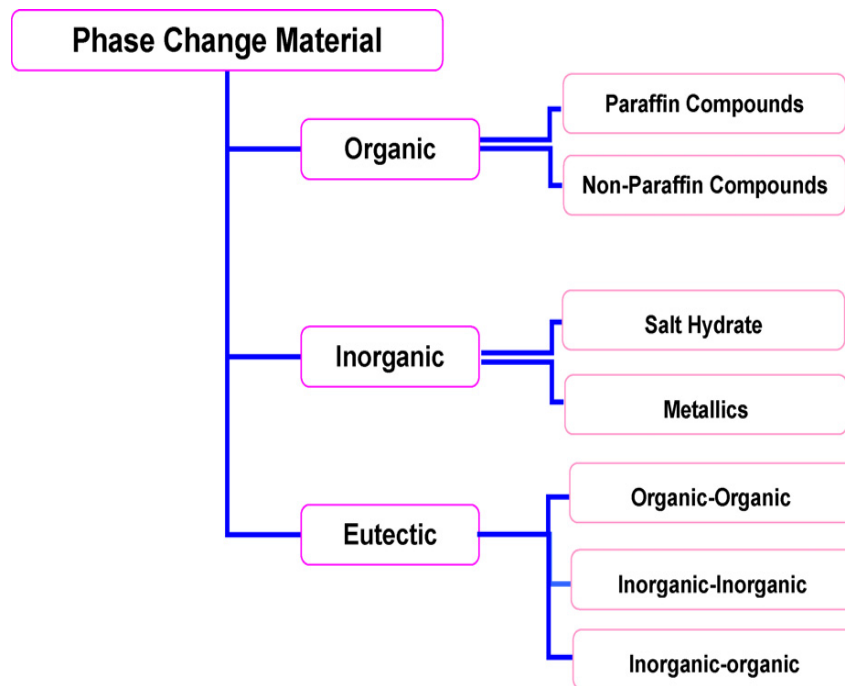


Fig 1. Classification of phase change materials [4]

### 1.2.1. *Inorganic PCM*

Salt hydrates and metallics make a group of phase change materials known as inorganic PCM. Salt hydrates are water containing inorganic salts resulting into the formation of a crystalline solid of general formula  $(AB_nH_2O)$ . Metallics include the metals and metal-eutectics melting at low temperature. Inorganic PCMs have following properties

- i. High latent heat of fusion on the volumetric basis
- ii. Higher thermal conductivity as compared to organic PCMs.
- iii. Negligible volume changes on melting.

However, apart from the above advantages, inorganic PCMs are toxic and corrosive. Any irreversibility in the process decreases the overall storage efficiency of the inorganic PCM.

### 1.2.2. Organic PCM

Organic PCMs are carbon-hydrogen based PCMs which are further described as paraffin and non-paraffins. Paraffin wax is a straight chain n-alkane represented by the formula  $\text{CH}_3\text{--}n(\text{CH}_2)\text{--CH}_3$ . Due to the crystallization of the  $(\text{CH}_2)$ -chain, a large amount of latent heat is released. As the length of the chain increases, the latent heat of fusion also increases along with the increase in the melting point. Since various paraffins are available with different melting temperatures, they can be used efficiently for energy storage over a large temperature range due to their high latent heat.

The non-paraffin organic PCMs consist of carbohydrates and fatty acids. They are the most numerous of the phase change materials with highly varied properties. Compared to inorganic PCMs, organic PCMs are generally more stable, and due to the following characteristics, they are generally preferred over inorganic PCMs

- i. Congruent melting (meaning that melting and freezing can be done repeatedly without any consequences such as phase segregation and reduction of latent heat)
- ii. Non-corrosiveness.
- iii. Non-toxicity
- iv. No signs of supercooling

### 1.2.3. Eutectics

A eutectic is a mixture of two or more components which has a melting point lower than that of each component of the mixture. Each of the component melts and freezes congruently forming a mixture of the component crystals during crystallization. Segregation is never a consequence of melting and freezing of eutectics as they freeze to an intimate mixture of crystals, leaving no chance for the components to separate. Separation of components is rare as both components liquify simultaneously with melting.

## 1.3 Selection criteria for PCM

- i. Melting temperature of the PCM should be lower than the maximum temperature of the device.
- ii. High latent heat of fusion on the volumetric basis.
- iii. High specific heat to provide additional sensible heat storage.
- iv. High density.

- v. Chemically stable.
- vi. Reversible freeze/melt cycle.
- vii. Small volume change.
- viii. Nontoxic, non-corrosive, non-flammable, non-explosive.
- ix. High thermal conductivity.
- x. Easily available.
- xi. Cost effective.

Paraffin wax satisfies all the above criteria but the high thermal conductivity. Hence thermal conductivity enhancers are needed to fulfill the need for high thermal conductivity.

#### **1.4 Applications of PCM**

- i. Together with heatsinks, PCM can achieve excellent thermal management of electronic devices reducing the temperature by absorbing a massive amount of heat.
- ii. Latent heat thermal storage systems like heat pumps, solar engineering, and spacecraft thermal control systems can use phase change materials (PCM).
- iii. Various PCMs are used in Medical applications like transportation of blood, operating tables, hot-cold therapies, treatment of asphyxia, where the temperature is to be kept constant.
- iv. Storing energy with the help of PCM can be of great use as it has a high latent heat of fusion which has the ability to absorb high energy leading to its application in solar cooking, solar power plants, thermal energy storage, cold energy battery and cooling of heat and electrical engines, etc.
- v. PCMs are also used in textiles, i.e., is used in clothing.
- vi. In the case of a power failure to conventional cooling systems, PCMs minimize the use of diesel generators, and this can translate into enormous savings across thousands of telecom sites in tropics.

## 1.5 Review of literature

In recent years, enhancing the thermal performance of electronic devices by passive cooling with the help of phase change materials (PCM) has gained increasing popularity. Due to their high latent heat of fusion and a small change in volume during phase change, they can be effective for energy storage system. Because of these desirable characteristics of the phase change materials, various studies have been reported on PCM [1-21]. However, almost all PCMs have low thermal conductivity which acts as a hindrance for enhancing the thermal performance of a system. For increasing the thermal conductivity, various thermal conductivity enhancers (TCEs) can be used like metallic fins, foams, matrices, and nanoparticles. Several studies have been reported regarding the use of metallic fins as the thermal conductivity enhancer for the PCMs.

Hosseinizadeh et al. [1] investigated the performance of the heatsink with PCM experimentally and numerically. Their results show that a numerical method can be used in simulating the process of PCM melting in a heatsink. Also, their results show that increasing the height and the number of fins has a much effect on improving the performance of heatsink, but by increasing the thickness of the fins, only a low improvement in performance is seen.

Fok et al. [2] experimentally studied the cooling of portable hand-held electronic devices using n-eicosane as the phase change material (PCM) placed inside heatsinks with and without internal fins. They considered various number of fins (0, 3, 6), the effect of orientation of the device with varying power level (3 to 5 W) on the transient thermal performances. Their results showed that heatsinks with internal fins containing PCM could be a viable option for cooling electronic devices but depending on various parameters like the number of fins, type of PCM, etc. further optimization is required.

Arshad et al. [3] analyzed round pin-finned heatsinks with paraffin wax as the phase change material (PCM). The pin fins which acted as the thermal conductivity enhancers (TCEs) were 9% of the total heatsink volume with 2mm, 3mm, and 4mm diameter. The results showed that the heatsink with 3mm pin fins diameter had the best thermal performance.

Arshad et al. [4] also analyzed passive cooling of electronic devices using rectangular pin-fin heatsink containing paraffin wax as the phase change material (PCM). Different pin-fin thickness was selected (1mm, 2mm, and 3mm) and their volume fraction was kept constant (9%). The results showed that the heatsink with 2mm pin fin thickness had the best thermal performance.

Baby and Balaji [5] investigated the thermal performance of pin-finned heatsinks containing n-eicosane as the phase change material (PCM). Different volume fractions of the pin fins were selected (4%, 9%, and 15%). Their results showed that heatsinks with fins were helpful in increasing the duration of operation of the electronic device. Heatsink with 9% pin fins showed the best result and increasing the number of fins beyond 9% resulted in reduced heat transfer enhancement.

For increasing the thermal conductivity of PCM, nanoparticles can also be used acting as TCE. Several studies have been investigated regarding nano-enhanced phase change material (NePCM), its preparation and characteristics and its effect on the thermal performance of a system.

Khodadadi and Hosseinizadeh [6] showed in their numerical study that the solidification time of the PCM can be significantly reduced with the increase of nanoparticles dispersion, and the composite of base PCM and nanoparticles was named ‘nano-enhanced phase change materials’ (NEPCM) in this study. Since then, NEPCM has attracted significant attention in the research community due to its great potential to store thermal energy.

Sharma et al. [7] investigated the phase change behavior of the nano-enhanced PCM containing palmitic acid as the PCM and nanoparticles of titanium dioxide (TiO<sub>2</sub>). The nanoparticles were dispersed into the palmitic acid in various mass fractions (0.5%, 1%, 3%, and 5%), and the corresponding increase in thermal conductivity of palmitic acid was seen (12.7%, 20.6%, 46.6%, and 80% respectively).

Ebrahimi et al. [8] numerically investigated the melting of a NePCM in a square cavity. They analyzed the impacts of the nanoparticle loading. They showed that by increasing the volume fraction of nanoparticles from 0 to 2%, the rate of melting would rise but by increasing it to 5%, melting rate is similar to that of pure PCM. The volumetric concentration of nanoparticles of 2% would result in the highest melting rate.

Krishna et al. [9] investigated the thermal performance of a heat pipe using nano-enhanced phase change material (PCM). Water and tricosane were used as the phase change materials. For the preparation of NePCM, nanoparticles of Al<sub>2</sub>O<sub>3</sub> were dispersed in tricosane with different volume percentages (0.5%, 1%, and 2%). It was found that the thermal conductivity of the PCM was enhanced up to a 32% of the pure tricosane with the help of nanoparticles. It was also found that the nano-enhanced PCM can store almost 30% of the total energy supplied.

Ho et al. [10] studied the effect of dispersing aluminium oxide ( $\text{Al}_2\text{O}_3$ ) nanoparticles in n-octadecane as the phase change material experimentally in a vertical square enclosure. Mass fractions of nanoparticles were 0%, 5% and 10%. Their results showed that with the increase in the mass fraction of nanoparticles in the nano-PCM, heat transfer due to natural convection decreases significantly when compared with that of the base PCM.

Aguila et al. [11] presented an experimental investigation about the behavior of thermal conductivity and viscosity of an O-PCM prepared from Octadecane and using Copper Oxide (CuO) as the nanoparticles. The nanoparticles were dispersed in different weight fractions (2.5%, 5%, and 10%). Sodium-oleate was used as the surfactant in order to increase the stability of the nanoparticles in the PCM and thus for uniform dispersion of nanoparticles. With the increase in the nanoparticle concentration, both thermal conductivity and viscosity were increased. Thermal conductivity was increased up to 9% with respect to the base fluid, and viscosity increased up to 60%.

Jethelah et al. [13] investigated a nano-PCM enclosure as thermal energy storage (TES) system experimentally and numerically. The effect of the volume fraction of CuO nanoparticles (0% to 5%) on coconut oil as the PCM was investigated. By adding nanoparticles, the melting process of the PCM was significantly improved.

Bayat et al. [14] numerically studied the performance of a finned heatsink with phase change material (PCM) and without PCM. With the use of PCM, the thermal performance of heatsink was improved as compared to that without PCM. Due to the low thermal conductivity of PCM, they also investigated the effect of the addition of copper oxide (CuO) and aluminium oxide ( $\text{Al}_2\text{O}_3$ ) nanoparticles on the paraffin wax as the PCM. The results showed that the heatsink performance was improved by adding a low percentage of nanoparticles (2%).

Bondareva et al. [15] investigated the heat transfer inside the finned heatsink filled with nano-enhanced n-octadecane. Their results showed that the addition of nanoparticles increases the melting rate at the initial stage of melting as the nanoparticles increase the thermal conductivity of the PCM resulting in increased heat transfer due to conduction. But, the convective heat transfer increases with time. Also, with increasing the fins length, the heat transfer became more efficient.

Shokouhmand et al. [16] investigated the heat transfer characteristics of lauric acid in a rectangular enclosure. In order to calculate the melt front, photographs were taken periodically, and with the help of MATLAB, the melt fraction was calculated by converting the image into

a binary image. Results showed that at the initial stage, heat transfer was mainly due to conduction and the convection heat transfer increased with time.

## 1.6 Objective

Current investigation focuses on the effect of dispersion of nanoparticles in the heatsink filled with phase change material on its thermal performance. Here paraffin wax is filled in a heatsink of dimensions 100mm×100\*20mm as phase change material, and Al<sub>2</sub>O<sub>3</sub> nanoparticles are added as the TCE. A heat plate is incorporated under a heatsink providing the constant heat flux of 2 kW/m<sup>2</sup>. Keeping heat flux constant, the effect of adding nanoparticles in different wt. fraction ( $\phi=0\%$ , 0.5%, 4%, and 6%) with the combination of 3 heatsinks on the thermal performance, melting time and melting front is studied.

The specific objectives of the current study are detailed below

1. Design and development of test facility to study the effect of dispersion of nanoparticles in the heatsink filled with phase change material on the thermal performance.
2. Conducting experiments for varied range of weight fractions ( $\phi=0\%$ , 0.5%, 4% & 6%) of nanoparticles with constant heat flux of 2 kW/m<sup>2</sup>.
3. Conducting experiments on varieties of heatsink enclosure as detailed below:
  - a) Heatsink without fin
  - b) Heatsink with one fin at midplane
  - c) Heatsink with two identical fins which are symmetrical from midplane.

## Chapter 2

### Experimental Facility

#### 2.1 Preparation of Heatsinks

- i. Aluminium blocks of dimension  $100 \times 100 \times 25 \text{ mm}^3$  were used to prepare heatsinks.
- ii. The blocks were cut in the workshop in required dimensions.
- iii. Then groove of 2mm depth was made by using 2mm wide end mill cutter on the milling machine.
- iv. Remaining work was carried in AMP (Advanced Manufacturing Process) lab, where it was reduced to required dimensions.
- v. Acrylic plates were used to cover sides of aluminium to form heatsinks.
- vi. The heatsink was filled with PCM for checking the leakage.
- vii. A layer of silicone gel is applied over the joints of the heatsink to nullify the possibility of leakage.
- viii. Fig 2 shows the transition of aluminium block to heatsinks.
- ix. Fig 3 shows the actual heatsink photographs.

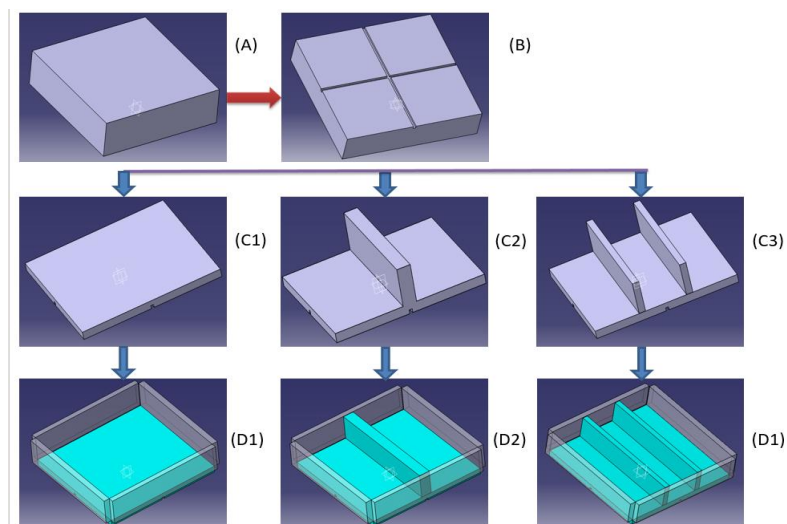


Fig 2. Preparation of heatsinks

A: Aluminium block, B: Groove on the face,  
C: Block reduced to required dimensions, D: Heatsink

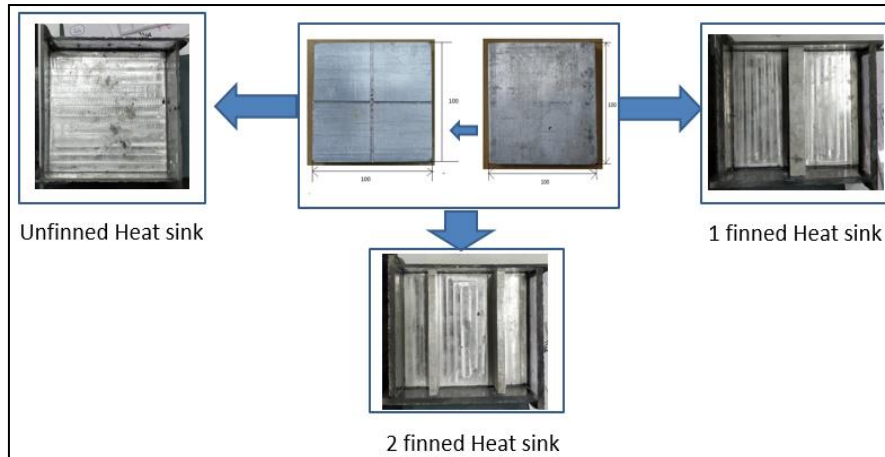


Fig.3 Photographic view of heatsinks

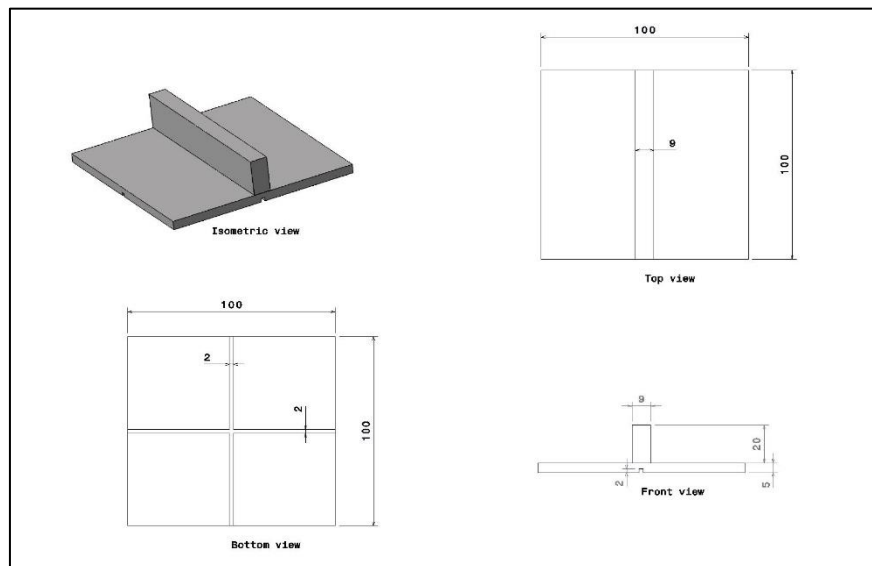


Fig 4. Detailed view of 1 finned heatsink

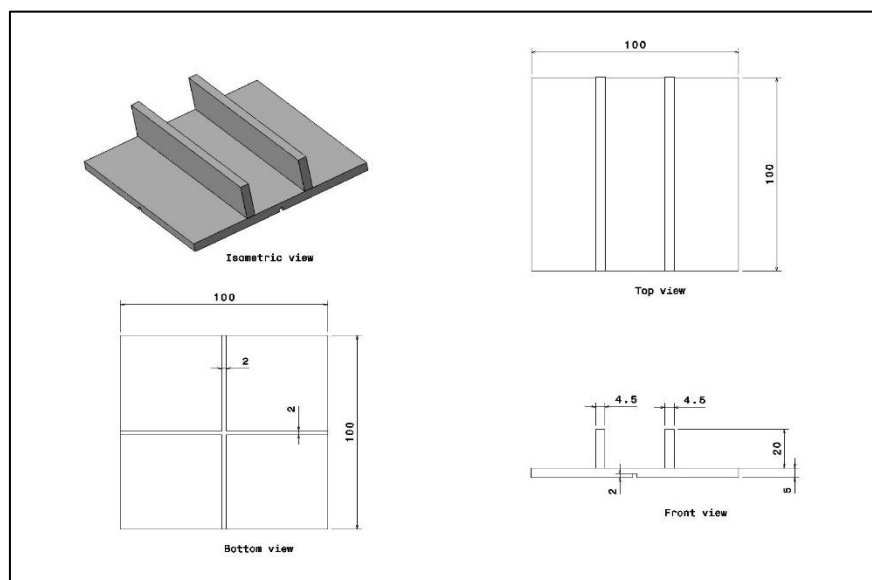


Fig 5. Detailed view of 2 finned heatsink

## 2.2 Locations of Thermocouples

The following figure shows the schematic of the locations of thermocouples. K type thermocouples are used in the present investigation, because of its wide range of temperature detection and good accuracy.

- i. Total of 12 thermocouples were located inside heatsink filled with NePCM.
- ii. Thermocouples were fixed at different heights from the base to check the temperature distribution.
- iii. 2 thermocouples T1 and T12 were placed at a distance of 5mm from the base of the heatsink.
- iv. 4 thermocouples T2, T5, T11, T8 were placed at a distance of 10 mm from the base of the heatsink
- v. 4 thermocouples T3, T6, T7, T10 were placed at a distance of 15mm from the base of the heatsink
- vi. 2 thermocouples T4 and 9 were placed at a distance of 5mm from the base of the heatsink.
- vii. Geometry is considered to fulfill the requirement of symmetry.

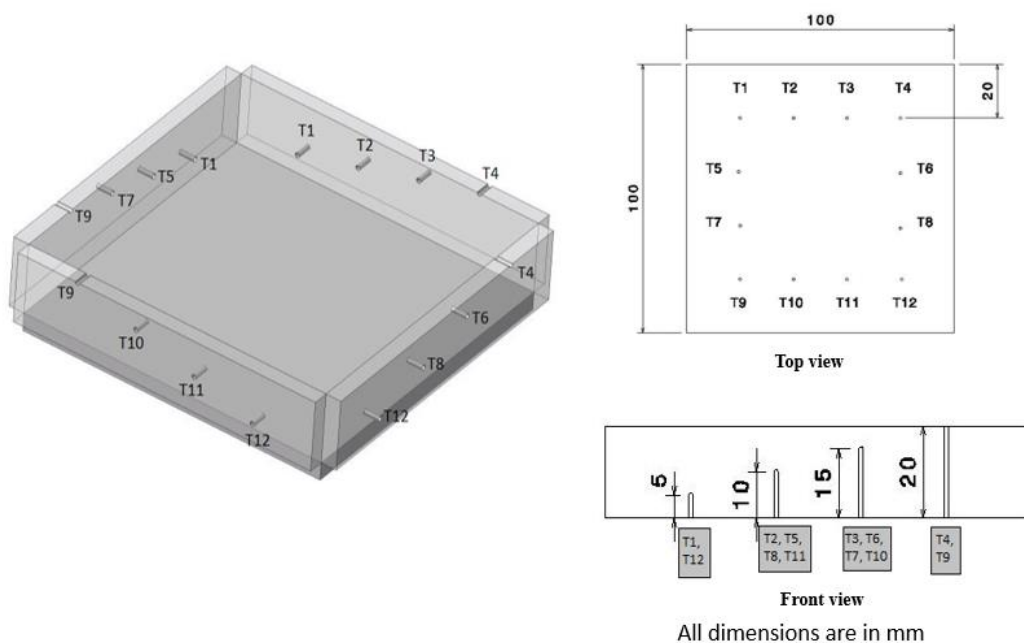


Fig 6. Locations of thermocouples in the heatsink.

Properties	Paraffin Wax		Aluminium (TCE)	Al <sub>2</sub> O <sub>3</sub> Nanoparticles	Acrylic (Insulator)
	Solid	Liquid			
Melting Temperature (°C)	58		660.37	-	-
Specific Heat (kJ/kg-K)	2.89	2.89	0.896	.765	1.470
Density (kg/m <sup>3</sup> )	900	750	2719	3600	-
Thermal Conductivity (W/m-K)	0.21	0.12	218	36	0.19
Latent Heat of Transformation (kJ/kg-K)	194.2		-	-	-

Table 1. Thermophysical properties of Paraffin wax, TCE and Insulator

### 2.3 Preparation of nano-enhanced PCM

Fig 4 shows the setup for the preparation of NePCM. According to the volume of the heatsink, the required amount of solid paraffin wax and Al<sub>2</sub>O<sub>3</sub> nanoparticle was weighed on Wensar PGB 301 machine. After weighing paraffin wax and Al<sub>2</sub>O<sub>3</sub> nanoparticles, solid paraffin wax is taken and melted using heat-plate at 75°C in a beaker. Al<sub>2</sub>O<sub>3</sub> nanoparticles are added periodically into the melted PCM while it is being stirred on the magnetic stirrer (REMI 2mlh) up to 2 hours. Then the mixture is sonicated for 2 hours at constant frequency with the help of ultrasonic vibrator (RICO Scientific Industries, USBT 6) for ensuring uniform distribution of nanoparticles in the PCM. Then the mixture is allowed to be cooled at room temperature.

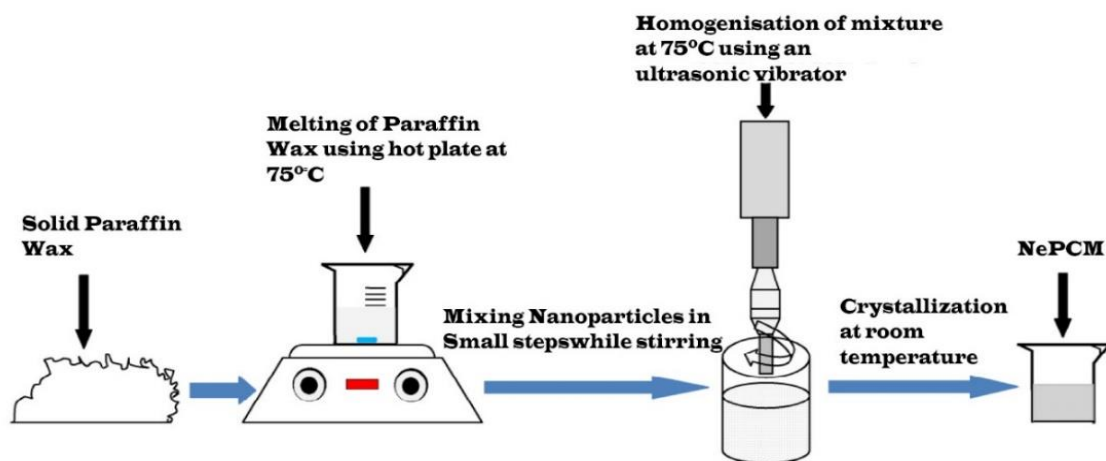


Fig 7. Schematic diagram for the preparation of NePCM [7]

## 2.4 Setup to measure the thermal performance of a heatsink filled with NePCM

Fig 8 shows the schematic diagram of the experimental setup. Firstly, heatsink is filled with NePCM, and acrylic plates are used to view the melt front of NePCM. The heatsink is placed above a heat plate of dimension  $100 \times 100 \times 4 \text{ mm}^3$ . Heat plate is attached to a DC source (APLab, Voltage range 0-30 v, Current range 0-4 A) for ensuring a constant heat flux of  $2 \text{ kW/m}^2$ . Insulation is provided to ensure no interactions with surroundings. Thermocouples (K type) are embedded in different locations in the heatsink as well as below it, to monitor the overall temperature distribution in the NePCM (Fig 8). Digital Camera (Sony Rx10, Resolution:  $1920 \times 1080$ , Pixel pitch: 2.41 micron, Sampling rate: 50fps) is used to view the melt front at the regular time intervals. Data Acquisition System (Agilent make 34972A, 32 channels) is used to process the data from thermocouples to record temperature values.

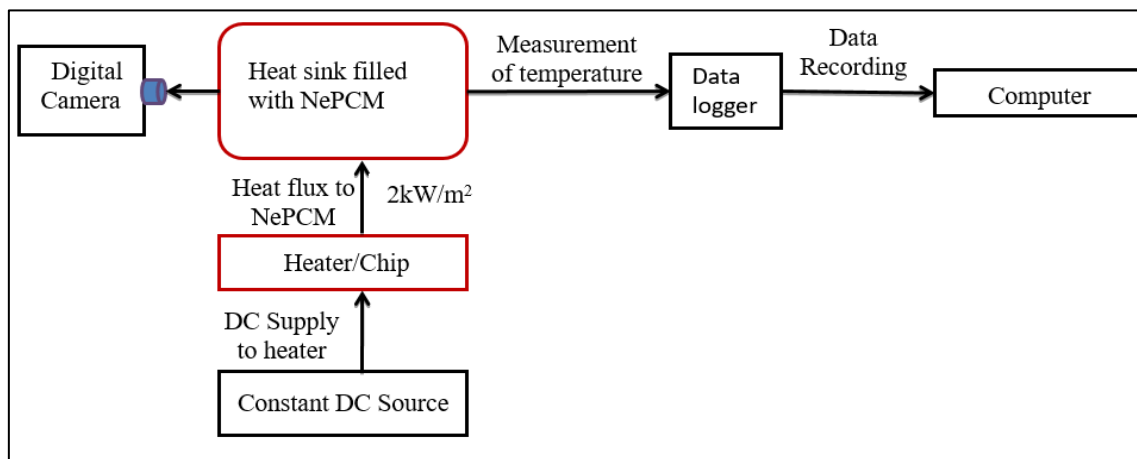


Fig 8. Schematic diagram of the experimental setup

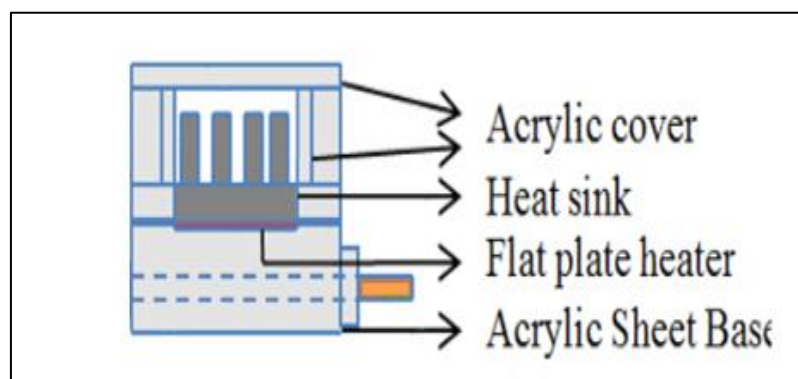


Fig 9. Detailed view of heatsink assembly

## Chapter 3

### Characterization and Data Processing

#### 3.1 DSC Characterization

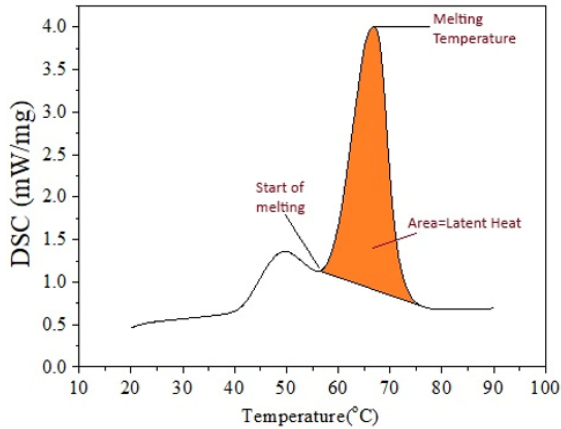


Fig 10. DSC curve of paraffin wax

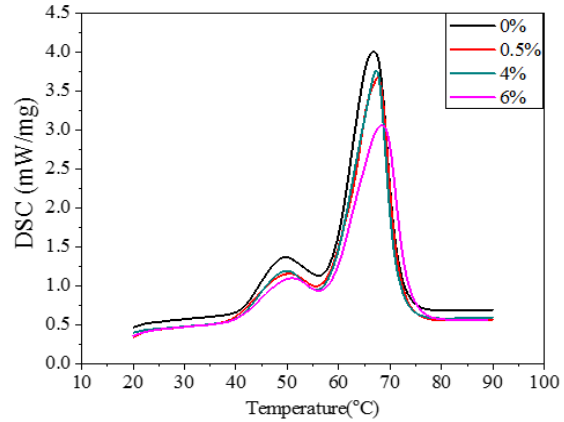


Fig 11. DSC curve for paraffin wax dispersed with different weight fractions of Al<sub>2</sub>O<sub>3</sub> Nanoparticles

The increment in temperature of the paraffin wax results in the loosened structure of PCM. Further increase causes the molecules to absorb the more heat, i.e., its latent heat, changing its phase to liquid, as absorbed energy gets converted into kinetic energy. Hence the measurements of the latent heat and melting temperature of the phase change materials are of extreme importance. The thermal energy storage properties of the pure paraffin wax and NePCMs of different Al<sub>2</sub>O<sub>3</sub> nanoparticle weight fractions are measured with the help of Differential Scanning Calorimetry analysis.

#### 3.2 SEM Characterization

Uniform dispersion is necessary for Scanning Electron Microscopy was done on all samples of PCM and NePCM to confirm uniform dispersion of nanoparticles. Fig 12 represents the FESEM image of NePCM taken on the Supra 55 Zeiss Field Emission Scanning Electron Microscope. Uniform dispersion of Al<sub>2</sub>O<sub>3</sub> nanoparticles can be seen in the figure. Hence it can be concluded that the use of magnetic stirrer to and ultrasonicator result in uniform dispersion of nanoparticles in the phase change material.

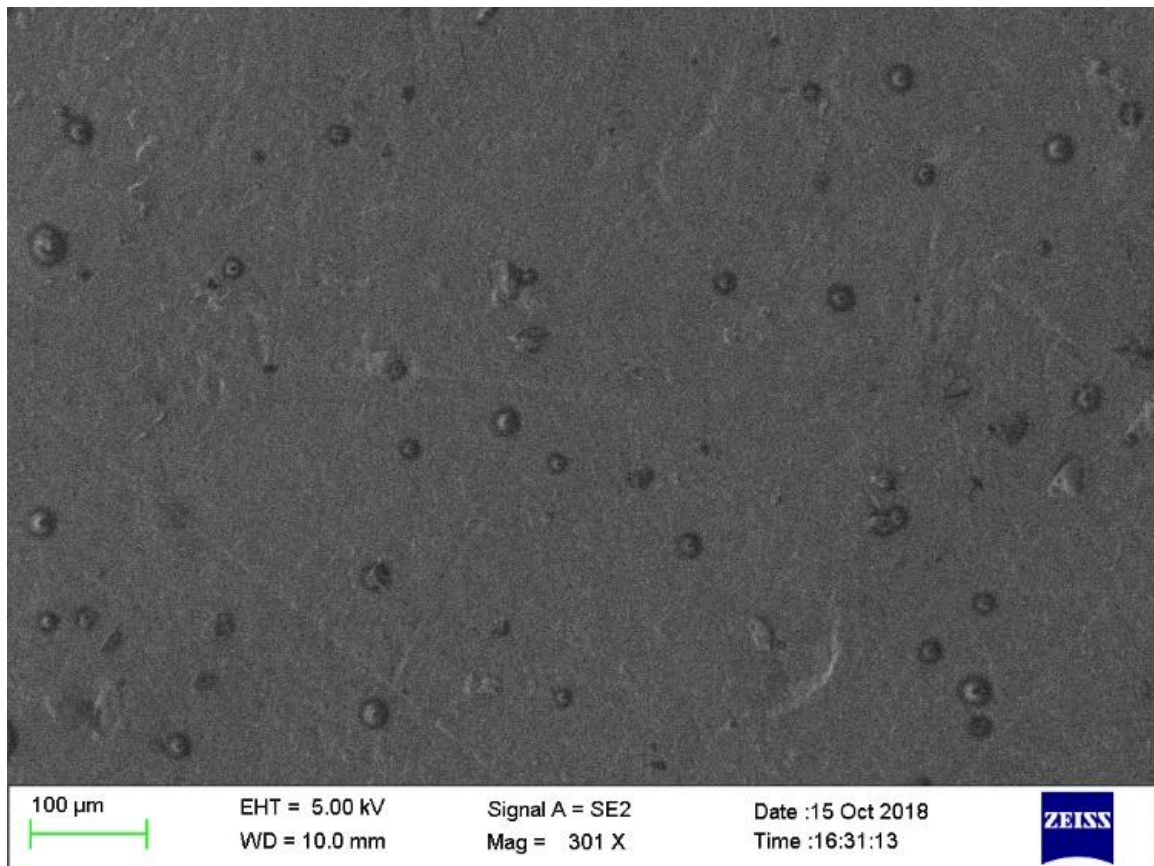


Fig 12. FESEM image of NePCM

### 3.3 Data processing

#### 3.3.1. Calculating melt fraction

The melt fraction was calculated with the help of images captured from one side of the heatsink (front side). The images captured were initially cropped to the required region which contained only the solid-liquid interface. After cropping and resizing them to appropriate size, they were enhanced. Photo enhancement made the solid-liquid interface clearly visible, and the melted portion was easily distinguishable from the solid wax. Then with the help of MATLAB, the enhanced images were converted into binary images. A binary image is a digital image whose pixels have only two possible intensity values (0 and 1). They are normally displayed as black and white, black corresponding the pixel having 0 value and white corresponding 1 value. Due to the photo enhancement, the melted portions were appropriately designated with the 0 value pixel (black pixels) and with proper code, the melt fraction was calculated by the number of pixels corresponding to the 0 value (black pixels) divided by the total number of pixels of the image.

$$\text{Melt fraction} = \frac{\text{Number of black pixels}}{\text{Total number of pixels}}$$

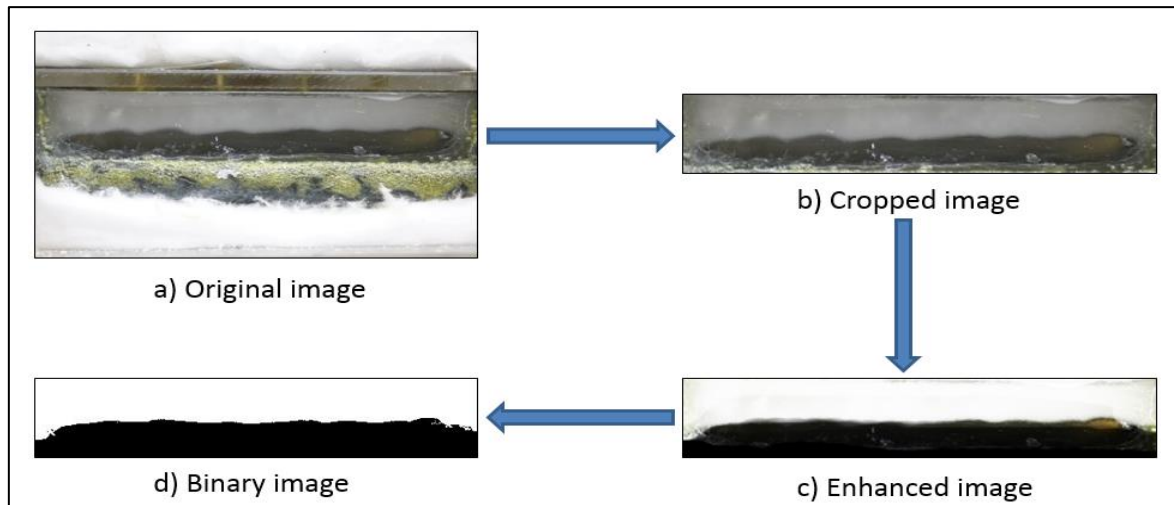


Fig 13. Steps involved in image processing to obtain the melt fraction for unfinned heatsink

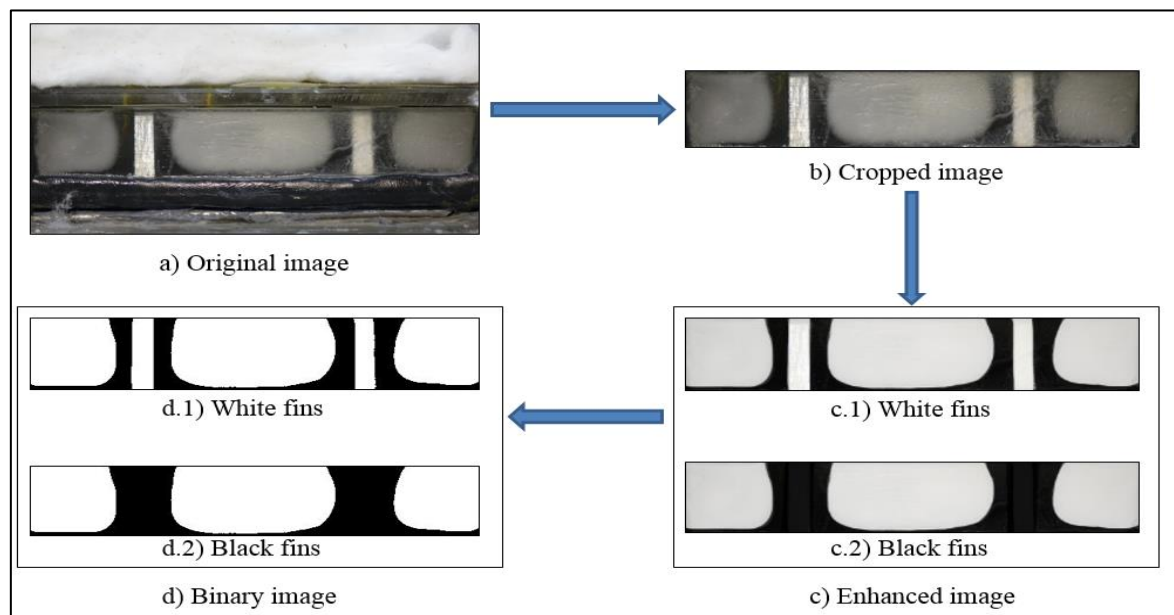


Fig 14. Steps involved in image processing to obtain the melt fraction for 2 finned heatsink

In case of finned heatsinks, it is necessary to exclude the portion where the pixels are of fins. In order to exclude the fin pixels, the cropped images are enhanced into two separate images.

One enhanced image contained the fins in white colour (c.1) and the other contained fins in black colour (c.2). The two enhanced images (c.1) and (c.2) are converted into binary images (d.1) and (d.2) respectively using MATLAB in the way similar to the images of unfinned heatsinks. The image (d.1) contained the black pixels of only liquid PCM, and the image (d.2) contained the white pixels of only solid PCM. To calculate the melt fraction, the number of black pixels from the image (d.1) was divided by the sum of number of black pixels from the image (d.1) and the number of white pixels from the image (d.2).

$$\text{Melt fraction} = \frac{\text{Black pixels of (d.1)}}{\text{Black pixels of (d.1) + White pixels of (d.2)}}$$

## Chapter 4

### Results and Discussions

#### 4.1 Comparison curves

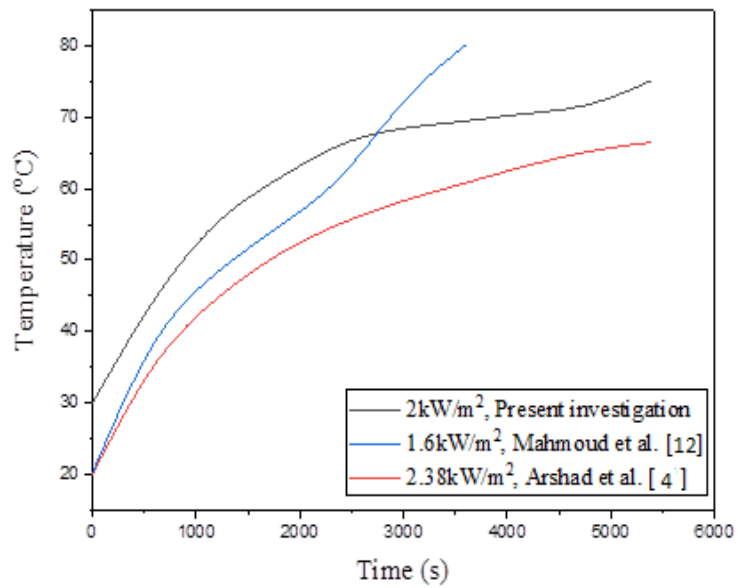


Fig 15. Comparison of present investigation with existing studies

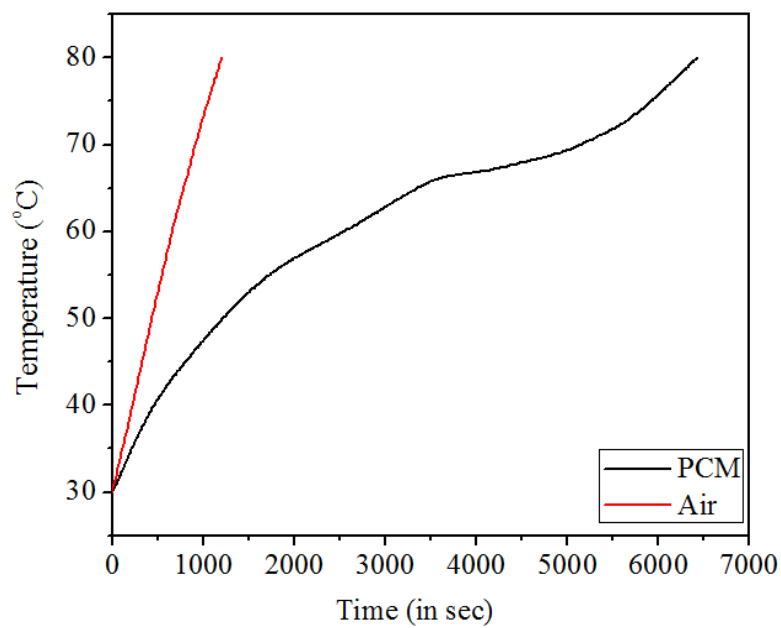


Fig 16. Comparison of the base temperature of 2 finned heatsink with and without PCM

Figure 15 shows the comparison between present investigations and previous investigations. A similar pattern is followed in the graph hence we can conclude that results in the present investigation are correct.

From the above Fig 16, it can be seen that adding PCM in the heatsink delays the time required to reach SPT (80°C) by 393% as compared to the air-based heatsink. Hence excellent thermal management can be achieved using a PCM based heatsink.

#### 4.2 Latent Heat Variation

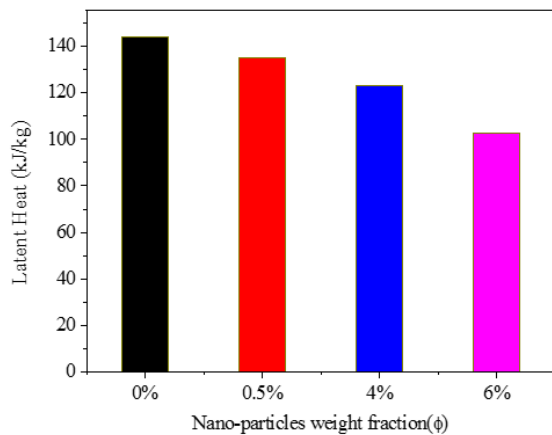


Fig 17. Variation of latent heat of PCM with nanoparticle loading

SAMPLE	Latent heat (J/g)	Variation in latent heat
PCM	143.8	0
$\phi = 0.5\%$	135	6.12%
$\phi = 4\%$	122.9	14.53%
$\phi = 6\%$	102.6	28.65%

Table 2. Variation of latent heat of PCM with nanoparticle loading.

Fig 10 & 11 shows the DSC curve for paraffin wax and nanoparticle added paraffin wax in different weight fractions. From Fig 11 it can be observed that the melting temperature variation is not significant after addition of external component, i.e., Al<sub>2</sub>O<sub>3</sub> nanoparticles. Reduction in the latent heat after addition of Al<sub>2</sub>O<sub>3</sub> nanoparticles can be seen in Fig 17 with maximum decrement being 28.65% for NePCM ( $\phi=6\%$ ). Dispersion of Al<sub>2</sub>O<sub>3</sub> nanoparticles causes changes in physiochemical properties of paraffin wax which results in the reduction of latent heat.

### 4.3 Propagation of melt front and variation of melt fraction with time

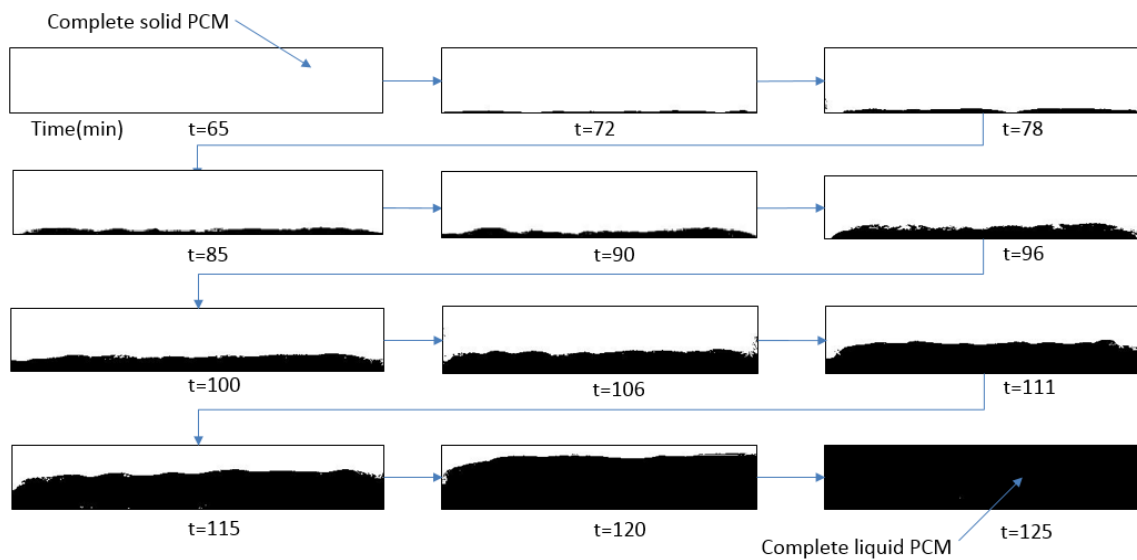


Fig 18. Progression of melt front of pure PCM ( $\phi=0$ ) for the unfinned heatsink

From the above figure, it can be seen that PCM starts to melt from the bottom of the heatsink and the melting of the PCM is horizontally layer by layer.

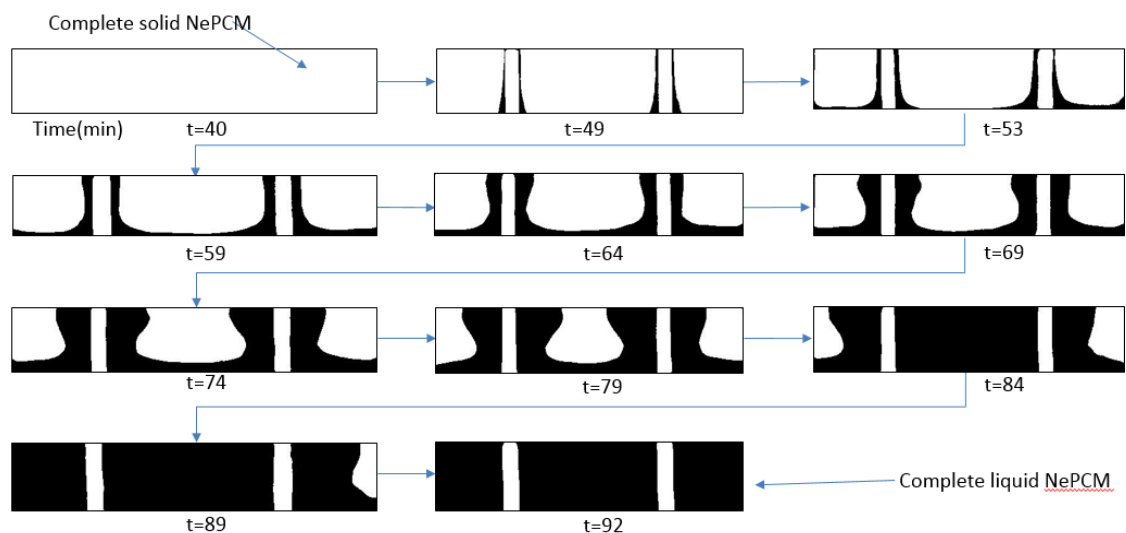


Fig 19. Progression of melt front of NePCM ( $\phi=4\%$ ) for the 2 finned heatsink

From the above figure, it can be seen that PCM starts to melt at the proximity of the fins and the melting of the PCM is not horizontally layer by layer as compared to that of the unfinned heatsink.

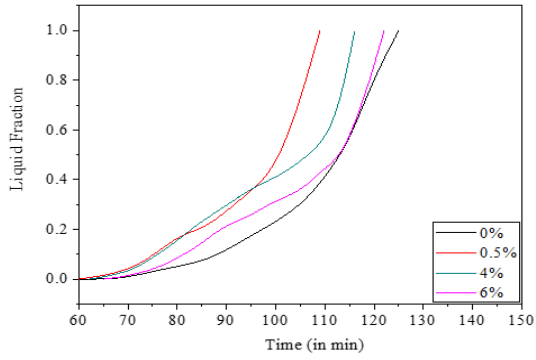


Fig 20. Variation of melt fraction with time for the unfinned heatsink

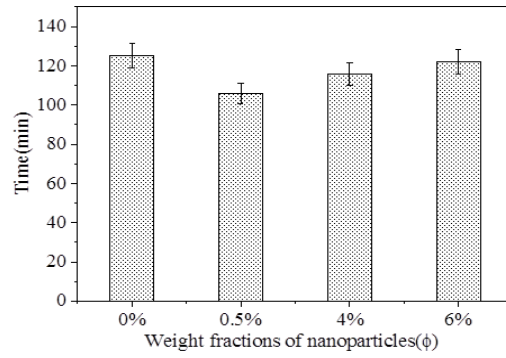


Fig 21. Melting time of NePCMs for the unfinned heatsink

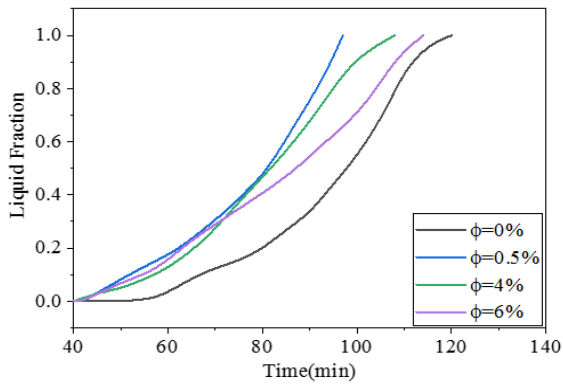


Fig 22. Variation of melt fraction with time for the 1 finned heatsink

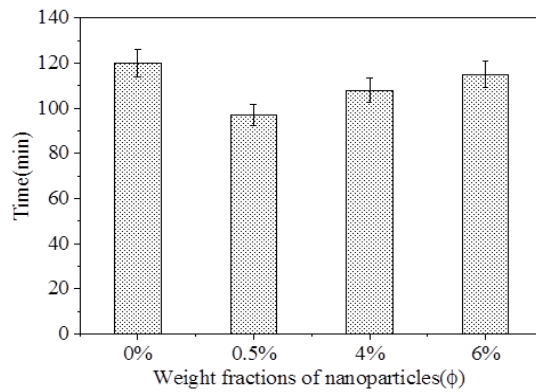


Fig 23. Melting time of NePCMs for the 1 finned heatsink

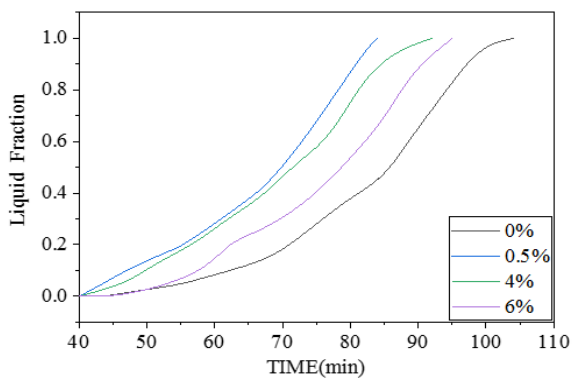


Fig 24. Variation of Melt fraction with time for the 2 finned heatsink.

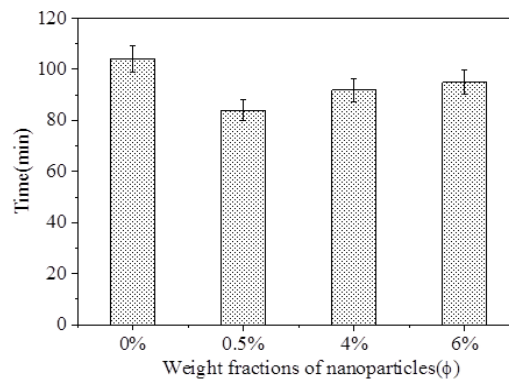


Fig 25. Melting time of NePCMs for the 2 finned heatsink

Fig 20, 22 and 24 shows the variation of melt fraction with time for different weight fractions ( $\phi$ ) of  $\text{Al}_2\text{O}_3$  nanoparticles dispersed in paraffin wax filled in unfinned and finned heatsinks (1 & 2 fins) and corresponding bar graphs (Fig 21, 23 and 25) shows the total melting time. In case of the unfinned heatsink, the melting starts early for NePCM compared to PCM due to increased thermal conductivity. NePCM ( $\phi=0.5\%$ ) melts faster than NePCM ( $\phi=4\%$  &  $6\%$ ). Highest melting time of 125 min was recorded for the PCM based heatsink and lowest melting time of 106 min was recorded for NePCM ( $\phi=0.5\%$ ). Maximum reduction of 15.23% in melting time was observed after the addition of 0.5%  $\text{Al}_2\text{O}_3$  nanoparticles. However, a further increase in nanoparticle loading causes an increase in melting time.

A similar pattern is observed in the case of 1 & 2 finned heatsink. NePCM ( $\phi=0.5\%$ ) gives the best results with the lowest melting time of 99 mins and 84 mins respectively. Melting time was increasing in order NePCM ( $\phi=0.5\%$ ), NePCM ( $\phi=4\%$ ), NePCM ( $\phi=6\%$ ), PCM. Maximum reduction of 17.5% and 19.23% in melting time was recorded after the addition of 0.5%  $\text{Al}_2\text{O}_3$  nanoparticles in 1 finned and 2 finned heatsinks respectively.

Melt fraction was higher for NePCM ( $\phi=4\%$ ) than NePCM ( $\phi=0.5\%$ ) at time 82 to 95 mins due to more thermal conductivity of NePCM ( $\phi=4\%$ ) as compared to NePCM ( $\phi=0.5\%$ ). Increase in melting time with nanoparticle loading is due to the increase in the viscosity and agglomeration.

#### 4.4 Effect of nanoparticle loading on heatsink base temperature

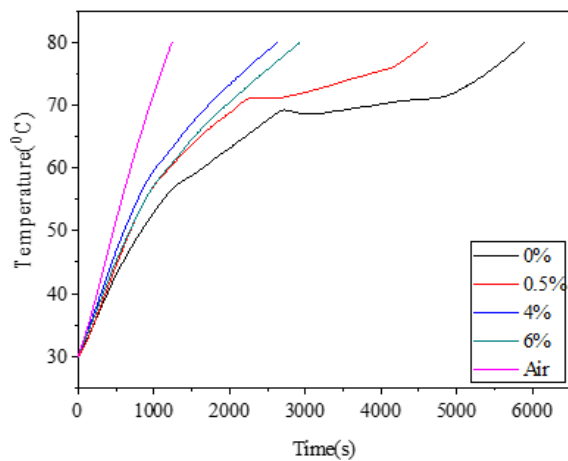


Fig 26. Variation of base temperature with time for unfinned heatsink.

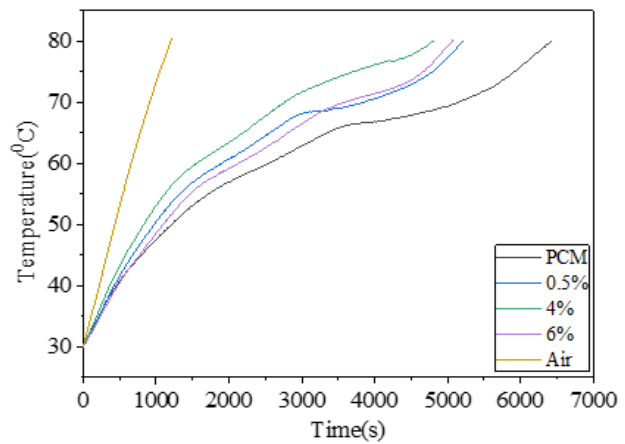


Fig 27. Variation of base temperature with time for 2 finned heatsink.

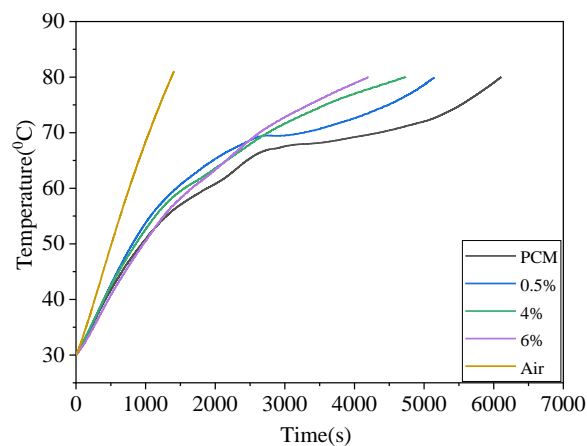


Fig 28. Variation of base temperature with time for 1 finned heatsink

Variation of the base temperature of the heatsink with time for different weight fractions of nanoparticles is shown in Fig 26, 27 & 28. More the time required to attain SPT better is the performance and thermal management of the system. Air-based heatsink reaches the 80 °C mark far early than PCM and NePCM based heatsinks. PCM based heatsink requires maximum time to reach SPT (80 °C). Hence its performance is best, followed by NePCM ( $\phi=0.5\%$ ) based heatsink. Further increment the nanoparticle loading results in a reduction of the thermal performance.

## Chapter 5

### Conclusions

Passive cooling thermal management technique using heatsinks filled with  $\text{Al}_2\text{O}_3$  nanoparticle dispersed paraffin wax has been implemented in this experiment. The effect of the addition of  $\text{Al}_2\text{O}_3$  nanoparticle in various weight fraction ( $\phi=0\%$ ,  $0.5\%$ ,  $4\%$ , and  $6\%$ ) in the paraffin wax filled in storage units with different dimensions on the thermal performance of the system has been analyzed. Experiments were performed for constant heat flux value of  $2 \text{ kW/m}^2$ . Melting process is observed photographically, and thermocouples were used to determine the temperature distribution inside the heatsinks. Photographs were captured at regular time intervals to view the melt front and Melt fraction has been determined by processing the captured photographs in the MATLAB software.

The key finding obtained from the present investigation are as follows

- i. Latent heat decreases with increase in the nanoparticle loading, maximum decrement being 28.65% for NePCM ( $\phi=6\%$ ) as compared to pure paraffin wax.
- ii. Adding PCM in 1 finned heatsink increases the operating time required to reach the SPT by 346% compared to the heatsink without PCM
- iii. Addition of nanoparticles results in the reduction in melting time, the maximum reduction being 15.23%, 17.5% and 19.23% for NePCM ( $\phi=0.5\%$ ) in unfinned, 1 finned and 2 finned heatsink.
- iv. Melting time increases with the further addition of  $\text{Al}_2\text{O}_3$  nanoparticles but it is still less as compared to pure PCM. A similar pattern is followed for 1 finned and 2 finned heatsinks.
- v. Pure PCM based heatsinks show the maximum delay in time to reach SPT ( $80^\circ\text{C}$ ).
- vi. Hence implementation of PCM based heatsinks in continuous operating electronic devices will be preferable to achieve excellent thermal management.
- vii. However, the addition of small amounts of nanoparticles will be essential as nano-enhanced PCM based heatsink will perform better in power spikes condition, and its installation in intermittent operating electronic devices will ensure better thermal management.

## References

1. S. Hosseinizadeh, F. Tan, S. Moosania, Experimental and numerical studies on the performance of PCM-based heatsink with different configurations of internal fins, *Applied Thermal Engineering*, 31 (2011), 3827-3838.
2. S. Fok, W. Shen, F.Tan, Cooling of portable hand-held electronic devices using phase change materials in finned heatsinks, *International Journal of Thermal Sciences*, 49 (2010), 109–117.
3. A. Arshad, H. Ali, Experimental investigation of PCM based round pin-fin heatsinks for thermal management of electronics: Effect of pin-fin diameter, *International Journal of Heat and Mass Transfer*, 117 (2018) 861–872.
4. A. Arshad, H. Ali, Thermal Performance of Phase Change Material (PCM) based Pin-Finned Heatsinks for Electronics Devices, *Applied Thermal Engineering*, 112 (2017) 143-155.
5. R. Baby, C. Balaji, Thermal management of electronics using phase change material based pin fin heatsinks, 395 (2012) 012134.
6. J. Khodadadi, S. Hosseinizad, Nanoparticle-enhanced phase change materials (NEPCM) with great potential for improved thermal energy storage, *International Communications in Heat and Mass Transfer*, 34 (2007), 534–543.
7. R. Sharma, P. Ganesan, Thermal properties and heat storage analysis of palmitic acid-TiO<sub>2</sub> composite as Nano-enhanced organic phase change material (NEOPCM), *Applied Thermal Engineering*, 99 (2016), 1254–1262.
8. A. Ebrahimi, A. Dadvand, Simulation of melting of a nano-enhanced phase change material (NePCM) in a square cavity with two heat source–sink pairs, *Alexandria Engineering Journal*, 54, 1003–1017.
9. J. Krishna, P. Kishore, Heat pipe with Nano enhanced-PCM for electronic cooling application *Experimental Thermal and Fluid Science*, 81 (2017), 84–92.
10. C. Ho, J. Gao, An experimental study on melting heat transfer of paraffin dispersed with Al<sub>2</sub>O<sub>3</sub> nanoparticles in a vertical enclosure, *International Journal of Heat and Mass Transfer*, 62(2013), 2-8.
11. B. Águila, D. Vasco, Effect of temperature and CuO-nanoparticle concentration on the thermal conductivity and viscosity of an organic phase-change material, *International Journal of Heat and Mass Transfer*, 120 (2018), 1009–1019.

12. S. Mahmoud, A. Tang, Experimental investigation of inserts configurations and PCM type on the thermal performance of PCM based heatsinks, *Applied Energy*, 112 (2013) 1349–1356.
13. M. Al-Jethelah, S. Tasnim, Nano-PCM filled energy storage system for solar-thermal applications, *Renewable Energy*, 126 (2018) 137-155.
14. M. Bayat, M. Faridzadeh, Investigation of finned heatsink performance with nano enhanced phase change material (NePCM), *Thermal Science and Engineering Progress*, 5 (2018), 50–59.
15. N. Bondareva, B. Buonomob, Heat transfer inside cooling system based on phase change material with alumina nanoparticles, *Applied Thermal Engineering*, 144 (2018), 972–981.
16. H. Shokouhmand, B. Kamkari, Experimental investigation on melting heat transfer characteristics of lauric acid in a rectangular thermal storage unit, *Experimental Thermal and Fluid Science*, 50 (2013) 201–212.
17. R. Kothari, S. Sahu, S. Kundalwal, Experimental investigations on thermal performance of PCM based heat sink for passive cooling of electronic components, *Proceedings of the 16th ASME International Conference on Nanochannels, Microchannels and Minichannels (ICNMM2018-7732)*, June 10-13, 2018, Dubrovnik, Croatia.
18. R. Kothari, S. Sahu, S. Kundalwal, Thermal management of electric vehicle battery modules with phase change materials, *Proceedings of the 24th National and 2nd International ISHMT-ASTFE Heat and Mass Transfer Conference (IHMTTC2017-15-0805)*, Dec 27-31, 2017, BITS Hyderabad, Telangana, India.
19. R. Kothari, S. Sahu, S. Kundalwal, Approximate analytical model for solidification process in a rectangular phase change material storage with internal fins, *Proceedings of 6th International Conference on Advances in Energy Research (Paper72)*, December 12-14, 2017, IIT Bombay, Mumbai, India.
20. R. Kothari, S. Kundalwal, S. Sahu, Transversely isotropic thermal properties of carbon nanotubes containing vacancies, *Acta Mech* 2018
21. R. Kothari, S. Sahu, S. Kundalwal, Comprehensive analysis of melting and solidification of a phase change material in an annulus, *Heat and Mass Transfer*

## **Publications**

1. R. Kothari, V. Shelke, D. Vaidya, S. Sahu, S, Kundalwal, Experimental investigation of thermal performance of nano-enhanced phase change materials for thermal management of electronic components, ASME 2019 Power Conference and Nuclear Forum, ASME 2019-1883.  
(Abstract submitted)

## Appendix

MATLAB was used for processing of images captured at a constant interval of time, to obtain the melt fraction at that time.

Following code was used to calculate the melt fraction of PCM and NePCM filled in the unfinned heatsink:

```
clc;
clear all;
folder='F:\Studies\BTP\Cropped\0%\Photoshop edited';
filenames=dir(fullfile(folder, '*.jpg'))
total=numel(filenames);
A=[1:total];
B=[1:total];
for n=1:total
f=fullfile(folder, filenames(n).name);
our_images=imread(f)
binary=im2bw(our_images);
figure, imshow(binary);
A(n)=numel(binary);
B(n)=sum(binary(:));
C(n)=A(n)-B(n);
D(n)=C(n)/A(n);
end
```

Following code was used to calculate the melt fraction of PCM and NePCM filled in the finned heatsinks

```
clc;
clear all;
folder1='F:\Studies\BTP\photos\1 Fin\4%\White';
filenames1=dir(fullfile(folder1, '*.jpg'))
total1=numel(filenames1);
```

```

A=[1:total1];
B=[1:total1];
for n=1:total1
    f1=fullfile(folder1, filenames1(n).name);
    our_images1=imread(f1)
    binary1=im2bw(our_images1);
    figure, imshow(binary1);
    A(n)=numel(binary1);
    B(n)=sum(binary1(:));
    C(n)=A(n)-B(n);
    imwrite(binary1,sprintf('%d.jpg',n));
end
folder2='F:\Studies\BTP\photos\1 Fin\4%\Black';
filenames2=dir(fullfile(folder2, '*.jpg'))
total2=numel(filenames2);
A=[1:total2];
B=[1:total2];
for n=1:total2
    f2=fullfile(folder2, filenames2(n).name);
    our_images2=imread(f2)
    binary2=im2bw(our_images2);
    figure, imshow(binary2);
    D(n)=sum(binary2(:));
    imwrite(binary2,sprintf('%d.jpg',100*n));
end
for i=1:total2
    E(i)=C(i)/D(i);
end

```